Requirements for the Tilted TTF Bypass Line

Georg Hoffstaetter*, DESY Hamburg, Germany

May 2001

Abstract

At TTF phase II there should be a bypass beam line around the undulators to the beam dump in order to avoid dumping the beam through the sensitive undulators. For this purpose a dipole in front of the collimator section bends the beam. For space reasons this bend will not be oriented exactly vertically upwards but slightly to the right. A second tilted dipole subsequently bends the beam back to make it parallel to the undulator beam line. The horizontal and vertical dispersion of the tilted dipoles which lead the beam into the bypass line should be compensated and therefore there have to be quadrupoles between the dipoles. One can either install quadrupoles which are not tilted and use them to compensate the horizontal and the vertical dispersion separately, or one can use quadrupoles which are tilted together with the dipoles and compensate the dispersion directly in the tilted dispersive plane of the dipoles. In this context the question of coupling comes up: How can a tilted beam line be constructed to produce a decoupled beam at its exit. Additionally the beta functions should not be too large.

Here general decoupling conditions are derived, the ellipse of the beam cross section for a coupled phase space is computed and it is shown that it is very similar to the uncoupled beam ellipse in shape but along the tilted beam line it is rotated significantly out of the horizontal plane. Different options for decoupling the horizontal and vertical motion will be investigated. The option with quadrupoles which are tilted together with the dipoles will proof superior and will be analyzed in more detail.

1 Decoupling Requirements for Tilted Beam Lines

The transfer matrix $\underline{M}_\varphi$ of a beam transport which is tilted by an angle φ is given by the rotation matrix $\underline{R}_\varphi$ and the transfer matrix $\underline{M}_0$ of the untilted beam line. The untilted beam line is assumed not to introduce coupling,

$$\underline{R}_\varphi = \begin{pmatrix} \cos\varphi\underline{1} & \sin\varphi\underline{1} \\ -\sin\varphi\underline{1} & \cos\varphi\underline{1} \end{pmatrix} , \quad \underline{M}_0 = \begin{pmatrix} \underline{M}_x & \underline{0} \\ \underline{0} & \underline{M}_y \end{pmatrix} , \tag{1.1}$$

*Georg.Hoffstaetter@desy.de

where $\underline{1}$ and $\underline{0}$ are the 2×2 unit and zero matrices respectively and

$$\begin{aligned} \underline{M}_\varphi &= \underline{R}_\varphi \underline{M} \underline{R}_{-\varphi} \qquad (1.2) \\ &= \frac{1}{2} \begin{pmatrix} \underline{M}_y + \underline{M}_x - \cos(2\varphi)(\underline{M}_y - \underline{M}_x) & \sin(2\varphi)(\underline{M}_y - \underline{M}_x) \\ \sin(2\varphi)(\underline{M}_y - \underline{M}_x) & \underline{M}_y + \underline{M}_x + \cos(2\varphi)(\underline{M}_y - \underline{M}_x) \end{pmatrix} . \end{aligned}$$

To avoid coupling in phase space at the exit of the tilted beam line, the beam spot after the tilted line is allowed to be rotated out of the horizontal by an angle θ, but the slopes in phase space have to be tilted by the same angle to decouple the phase space motion in a plane which is rotated by θ out of the horizontal. This avoids a blow up of the emittance when the following beam line magnets are tilted by θ and requires that the total matrix of the tilted beam line can be written as the product of a decoupled matrix and a subsequent rotation by θ:

$$\underline{M}_\varphi = \underline{R}_\theta \underline{A} , \quad \underline{A} = \begin{pmatrix} \underline{A}_x & \underline{0} \\ \underline{0} & \underline{A}_y \end{pmatrix} . \qquad (1.3)$$

In order to decouple, there must therefore exist a matrix $\underline{A}$ with

$$\begin{aligned} \underline{A} &= \underline{R}_{-\theta} \underline{R}_\varphi \underline{M} \underline{R}_{-\varphi} \qquad (1.4) \\ &= \frac{1}{2} \begin{pmatrix} \cos\theta(\underline{M}_y + \underline{M}_x) - \cos(2\varphi - \theta)(\underline{M}_y - \underline{M}_x) & \\ \sin\theta(\underline{M}_y + \underline{M}_x) + \sin(2\varphi - \theta)(\underline{M}_y - \underline{M}_x) & \\ & -\sin\theta(\underline{M}_y + \underline{M}_x) + \sin(2\varphi - \theta)(\underline{M}_y - \underline{M}_x) \\ & \cos\theta(\underline{M}_y + \underline{M}_x) + \cos(2\varphi - \theta)(\underline{M}_y - \underline{M}_x) \end{pmatrix} . \end{aligned}$$

This matrix can only have block diagonal form if $\sin\theta(\underline{M}_y + \underline{M}_x) = 0$ and $\sin(2\varphi - \theta)(\underline{M}_y - \underline{M}_x) = 0$. There are therefore the two following possibilities:

1. $\theta = 0$ and $\underline{M}_y = \underline{M}_x$.
2. $\theta = 2\varphi$ and $\underline{M}_y = -\underline{M}_x$.

2 The Beam Spot for a Coupled Optics

A decoupled Gaussian beam distribution is given by

$$\begin{aligned} \rho_0(\vec{z}) = \frac{1}{(2\pi\epsilon_x\epsilon_y)^2} \quad & \cdot \quad \exp(-\frac{1}{2\epsilon_x}[\beta_{x0}x'^2 + 2\alpha_{x0}xx' + \gamma_{x0}x^2]) \qquad (2.5) \\ & \cdot \quad \exp(-\frac{1}{2\epsilon_y}[\beta_{y0}y'^2 + 2\alpha_{y0}yy' + \gamma_{y0}y^2]) . \end{aligned}$$

This can be simplified to

$$\begin{aligned} \rho_0(\vec{z}) &= \frac{1}{(2\pi)^2\epsilon_x\epsilon_y} \exp(-\vec{z}^T \underline{\beta}_0 \vec{z}) , \quad \underline{\beta}_0 = \begin{pmatrix} \frac{1}{2\epsilon_x}\underline{\beta}_{x0} & \underline{0} \\ \underline{0} & \frac{1}{2\epsilon_y}\underline{\beta}_{y0} \end{pmatrix} \qquad (2.6) \\ \underline{\beta}_{j0} &= \begin{pmatrix} \gamma_{j0} & \alpha_{j0} \\ \alpha_{j0} & \beta_{j0} \end{pmatrix} , \quad j \in \{x, y\} . \qquad (2.7) \end{aligned}$$

After a coupled beam transport described by the matrix $\underline{M}$, the density is given by $\rho(\vec{z}) = \frac{1}{(2\pi)^2 \epsilon_x \epsilon_y} \exp(-\vec{z}^T \underline{\beta} \vec{z})$ with $\underline{\beta} = \underline{M}^{-T} \underline{\beta}_0 \underline{M}^{-1}$. The projection of this density onto the x–y plane describes the beam spot. It is given by

$$\rho_b(x,y) = \int_{-\infty}^{\infty} \int_{-\infty}^{\infty} \rho(\vec{z}) dx' dy' = \frac{1}{N} \exp(-(x,y)\underline{\sigma} \begin{pmatrix} x \\ y \end{pmatrix}) \; . \tag{2.8}$$

An evaluation of the integral leads to

$$\begin{aligned}
N &= \frac{1}{4\pi \epsilon_x \epsilon_y \sqrt{\beta_{22}\beta_{44} - \beta_{24}^2}} \qquad (2.9)\\
d &= \beta_{24}^2 - \beta_{22}\beta_{44} \; , \quad \sigma_{21} = \sigma_{21} \; , \\
\sigma_{11} &= \frac{1}{d}[\beta_{14}(\beta_{14}\beta_{22} - \beta_{12}\beta_{24}) + \beta_{12}(\beta_{12}\beta_{44} - \beta_{14}\beta_{24}) + \beta_{11}(\beta_{24}^2 - \beta_{22}\beta_{44})] \; , \\
\sigma_{22} &= \frac{1}{d}[\beta_{34}(\beta_{22}\beta_{34} - \beta_{24}\beta_{23}) + \beta_{23}(\beta_{23}\beta_{44} - \beta_{24}\beta_{34}) + \beta_{33}(\beta_{24}^2 - \beta_{22}\beta_{44})] \; , \\
\sigma_{12} &= \frac{1}{d}[\beta_{23}(\beta_{12}\beta_{44} - \beta_{24}\beta_{14}) + \beta_{34}(\beta_{14}\beta_{22} - \beta_{12}\beta_{24}) + \beta_{13}(\beta_{24}^2 - \beta_{22}\beta_{44})] \; .
\end{aligned}$$

The lines with equivalent density are tilted ellipses described by the eigenvalues λ_1 and λ_2 of the matrix $\underline{\sigma}$. Pseudo beta functions are introduced which characterize the size of the tilted ellipses by

$$\beta_x^\star = \frac{1}{2\epsilon_x \lambda_1} = \frac{1}{\epsilon_x} \cdot \frac{1}{\sigma_{11} + \sigma_{22} + \mathrm{sig}(\sigma_{11} - \sigma_{22})\sqrt{(\sigma_{11} - \sigma_{22})^2 + 4\sigma_{12}^2}} \; , \tag{2.10}$$

$$\beta_x^\star = \frac{1}{\epsilon_y \lambda_2} = \frac{1}{\epsilon_y} \cdot \frac{1}{\sigma_{11} + \sigma_{22} - \mathrm{sig}(\sigma_{11} - \sigma_{22})\sqrt{(\sigma_{11} - \sigma_{22})^2 + 4\sigma_{12}^2}} \; . \tag{2.11}$$

The sign function has been used to let $\beta_x^\star$ become β_x for a decoupled optics where σ_{12} is zero.

The orientation of the axis of the ellipse which corresponds to $\beta_x^\star$ has the angle Θ to the x axis which is given by the eigenvector to the eigenvalue λ_1,

$$\Theta = \mathrm{atan}(\frac{\sigma_{12}}{\lambda_1 - \sigma_{22}}) \; . \tag{2.12}$$

For decoupled motion Θ is always zero.

3 A Tilted Bypass Without Tilted Quadrupoles

Initially the different decoupling concepts were tested by assuming a small angle of 7° between the plane of the bypass and the vertical. The bends leading into the bypass were assumed to have 19° bend angle and a length of 1.2 m. Their centers where chosen to be 4 m apart. For these studies, the Twiss functions before the first dipole were set to the preliminary design values of

$$\beta_{x0} = 12.41\mathrm{m} \; , \quad \alpha_{x0} = 0.37 \; , \quad \beta_{y0} = 20.35\mathrm{m} \; , \quad \alpha_{y0} = -2.90 \tag{3.13}$$

and should not lead to exceedingly large beam sizes. After the bend section they were matched to a FODO structure in the bypass line. The influence of coupled phase space motion on the beam spot depends on the emittance ratio, and equal emittances $\epsilon_x = \epsilon_y$ will be assumed.

If the tilted dipole magnets would not introduce coupling, then one could use only horizontal quadrupoles in between the dipoles to guarantee that the optic of the complete bend section is decoupled. In this scheme at least four quadrupoles are required between the two dipoles in order to compensate the independent quantities D_x, $D_{x'}$, D_y, $D_{y'}$. It turns out that an additional quadrupole is required in order to keep the vertical betatron amplitude under control.

However, the tilted dipoles introduce coupling. If one for example chooses a parallel face magnet, which focuses in the vertical plane but not in the horizontal, then the focusing in the tilted plane introduces coupling which significantly disturbs the beta functions after the tilted bend section of the bypass. Nevertheless, the beta functions in the FODO section corresponding to the maximum horizontal and vertical amplitude of the beam spot computed by

$$\beta_{x,max} = \frac{\sigma_{22}}{\sigma_{11}\sigma_{22} - \sigma_{12}^2} \ , \quad \beta_{y,max} = \frac{\sigma_{11}}{\sigma_{11}\sigma_{22} - \sigma_{12}^2} \tag{3.14}$$

are quite similar to the periodic FODO beta functions as shown in figure 3.1. The optimizations of the coupled optics were performed with the code COSY INFINITY [1].

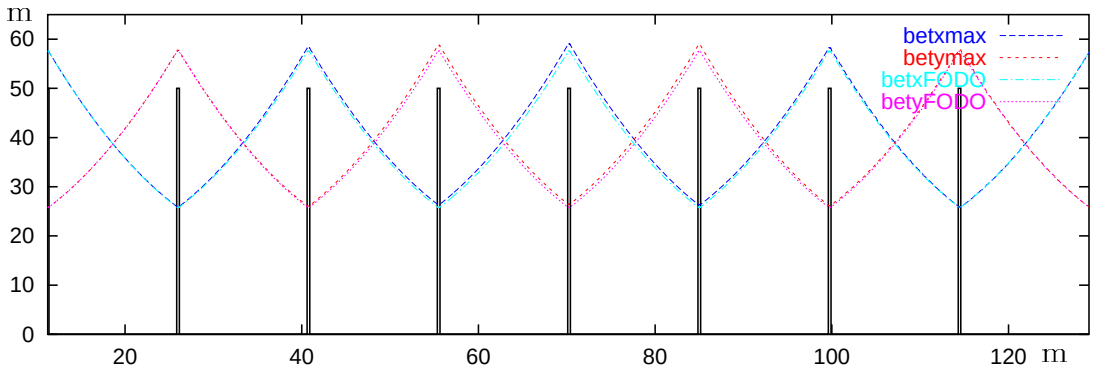

Figure 3.1: Beta functions corresponding to the maximum x and y coordinate of the beam spot for tilted parallel faced dipole magnets and horizontal quadrupoles compared to the matched beta functions of the FODO section.

But the pseudo beta functions and the tilt angle of the beam spot are significantly disturbed as shown in figure 3.2 for the bend section, for the subsequent matching section, and for the first two adjacent FODOs. The non–vanishing angle Θ of the beam spot orientation shows that the optic in the FODO section is not decoupled. This is reflected by the fact that the pseudo beta functions do not agree with the matched beta functions of the FODO structure.

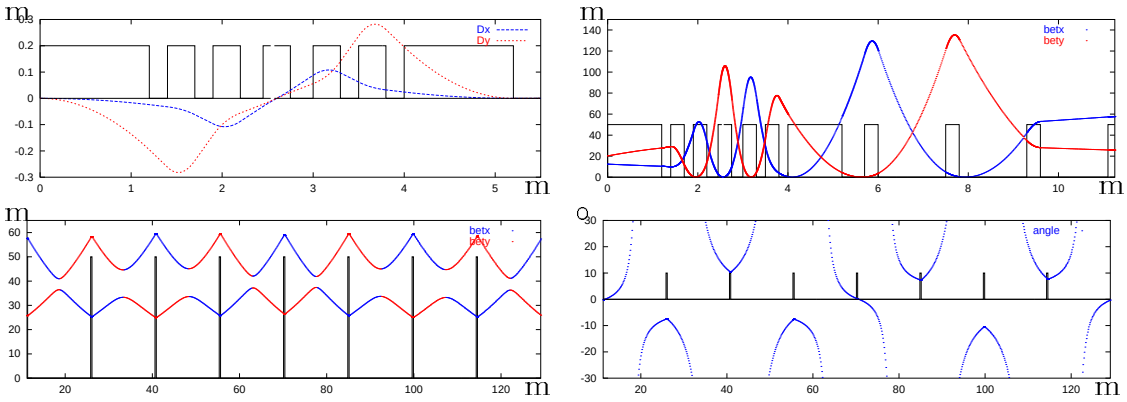

Figure 3.2: Pseudo beta functions of the coupling introduced by a tilted parallel faced dipole magnet and horizontal quadrupoles. 1: Dispersion correction, 2 and 3: pseudo beta functions, 4: Angle Θ of the beam spot orientation.

In the here described scheme in which the quadrupoles are all horizontal and only the dipoles are tilted, it is therefore important to minimize the coupling introduced by the tilted dipole. For a 1.5m long dipole with $\phi = 19°$, $\sum_{ij=1}^{4}(M_{xij} - M_{yij})^2$ is minimal for an entrance and exit edge of $\epsilon = 4.76°$. The corresponding beta functions are shown in figure 3.3. The matching condition have been: $D_x = 0$,

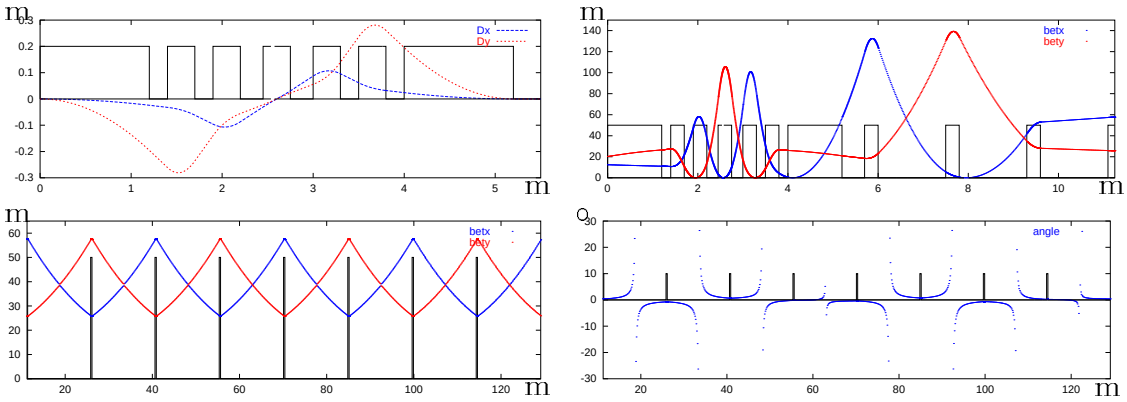

Figure 3.3: Pseudo beta functions of the coupling introduced by a tilted dipole magnet with 4.76° edge focusing and by $-0.4°$ tilted quadrupoles. 1: Dispersion correction, 2 and 3: pseudo beta functions, 4: Angle Θ of the beam spot orientation.

$D_{x'} = 0$, $D_y = 0$, $D_{y'} = 0$ after the second dipole and a match to a $l/2 = 17$m and 45° FODO at the entrance of the 9th quadrupole. The nearly vanishing angle Θ of the beam spot orientation shows that the optic in the FODO section is decoupled very well. The angle is only large in non–critical regions where the beam spot is nearly circular,i.e. at $\beta_x^\star = \beta_y^\star$ for $\epsilon_x = \epsilon_y$. This is reflected by the fact that the pseudo beta functions agree very well with the matched beta functions of the FODO structure.

A horizontal quadrupole here does not refer to a quadrupole for which the top and bottom edges are horizontal but to one which is by $-\varphi$ rotated with respect to the exit face of the first dipole. The top and bottom edges of these quadrupoles therefore have an angle of $\text{atan2}(\sin\varphi\cos\phi, \cos\varphi) - \varphi = -0.4°$ to the horizontal.

If one does chooses quadrupoles with horizontal edges, the optic is not as nicely decoupled. This is shown by the pseudo beta functions and the beam spot angle shown in figure 3.4. These horizontal quadrupoles are tilted by $\text{atan2}(\sin\varphi\cos\phi, \cos\varphi) = 82.6°$ with respect to the tilted quadrupoles of section 4 and the front and back faces are tilted by $\text{asin}(\sin\varphi\sin\phi) = 18.85\circ$ away from the vertical. The non–vanishing

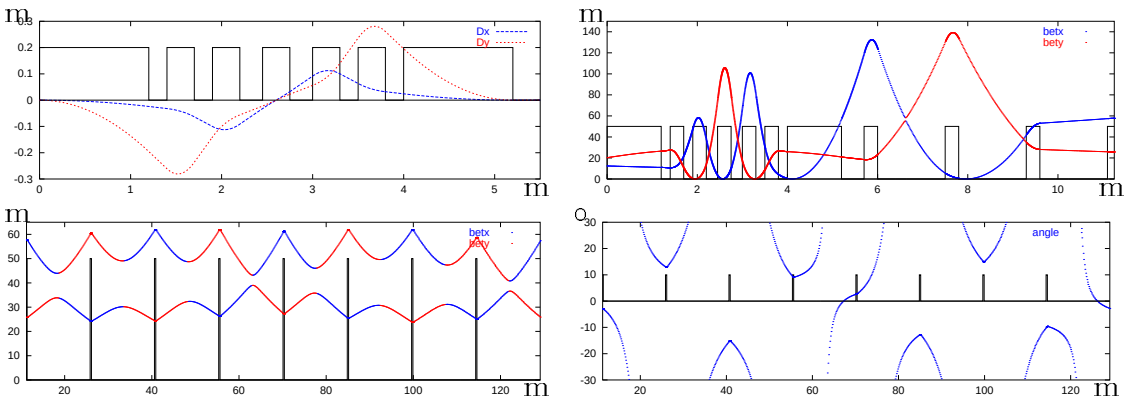

Figure 3.4: Pseudo beta functions of the coupling introduced by a tilted dipole magnet with 4.76° edge focusing and horizontal quadrupoles. 1: Dispersion correction, 2 and 3: pseudo beta functions, 4: Angle Θ of the beam spot orientation.

angle Θ of the beam spot orientation shows again that the optic in the FODO section is not decoupled. This is reflected by the fact that the pseudo beta functions do not agree with the matched beta functions of the FODO structure. But also here the beta function corresponding to the maximum horizontal and vertical amplitude of the tilted beam spot are quite similar to the decoupled beta functions as shown in figure 3.5. Therefore also this not completely decoupled arrangement with horizontal quadrupoles will most likely be sufficient for most purposes.

4 Decoupling with Tilted Quadrupoles

Quadrupoles have to be placed in between the two dipoles in order to produce vanishing D and D'. If the dipoles where not tilted by φ, this would require two horizontal quadrupoles. When the dipoles are tilted, the two quadrupoles also have to be tilted. Two tilted quadrupoles are then sufficient to compensate all four quantities D_x, $D_{x'}$, D_y, $D_{y'}$ since $D_y\cos\varphi = D_x\sin\varphi$. However, since both of these quadrupoles have to be focusing in the dispersive plane, it turns out that a third quadrupole is required to reduce the betatron amplitudes in the transverse plane. Additional tilted quadrupoles after the bend section would be needed in order to

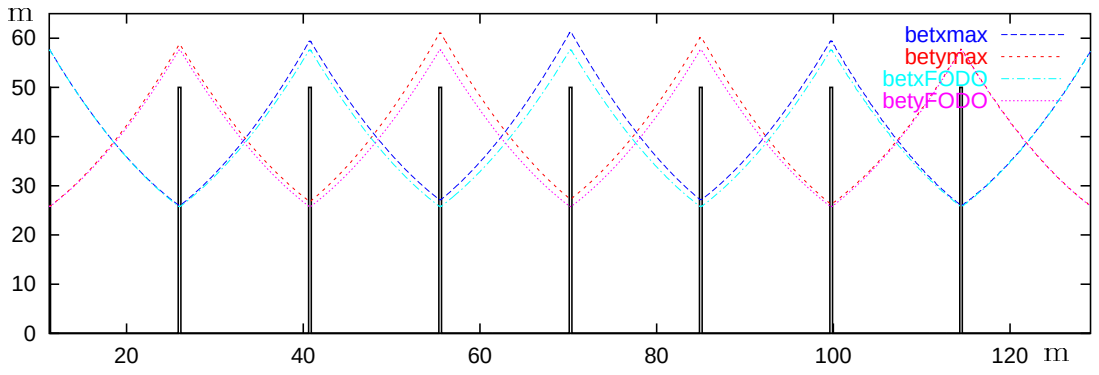

Figure 3.5: Beta functions corresponding to the maximum x and y coordinate of the beam spot for a tilted dipole magnet with 4.76° edge focusing and horizontal quadrupoles compared to the matched beta functions of the FODO section.

decouple the optics, i.e. to lead to a transfer matrix of the tilted section with either $\underline{M}_x = \underline{M}_y$ or $\underline{M}_x = -\underline{M}_y$.

Both cases have been analyzed. The case with $\underline{M}_x = -\underline{M}_y$ can be achieved with two tilted quadrupoles after the second dipole, but the four quadrupoles of the subsequent matching section and all following FODO quadrupoles would have to be tilted by $2\varphi = 14°$. To avoid this inconvenience, the condition $\underline{M}_x = \underline{M}_y$ has been adopted.

The case with $\underline{M}_x = \underline{M}_y$ requires 3 tilted quadrupoles after the second dipole but it has the advantage that all subsequent quadrupoles can be horizontal. The coupled pseudo beta functions and the tilt of the beam spot is shown in figure 4.6. In both of these cases the dipole magnets were assumed to be parallel faced magnets. Since the complete tilted section of the beam line is decoupled, no special decoupled dipole is required. For 0.3 m long quadrupoles, the maximum quadrupole strength in between the two dipoles is 9.5/m and for the matching section it is 4.5/m. The matching condition have been: $D_x = 0$, $D_{x'} = 0$ after second dipole, $\underline{M}_x = \underline{M}_y$ after 6th quadrupole, match to a $l/2 = 17$m and 45° FODO at the entrance of the 10th quadrupole. The vanishing angle Θ of the beam spot orientation shows that the optic in the FODO section is completely decoupled.

5 Nonlinear Optics

In order to find out whether it is the feasible to transport the emittances and energy spreads of the TTF beam with these optics, particles were tracked through the bypass option with 5 quadrupoles between the decoupled dipoles of section 3 and through that with 3 tilted quadrupoles of section 4. The chosen beam parameters are normalized emittances of $\epsilon_x = \epsilon_y = 2\pi$mm mrad and an energy spread of $\delta = 1 \cdot 10^{-3}$.

The tracking results are shown in figure 5.7. These figures show that the emittances would be blown up if no sextupoles were used to correct the energy depend-

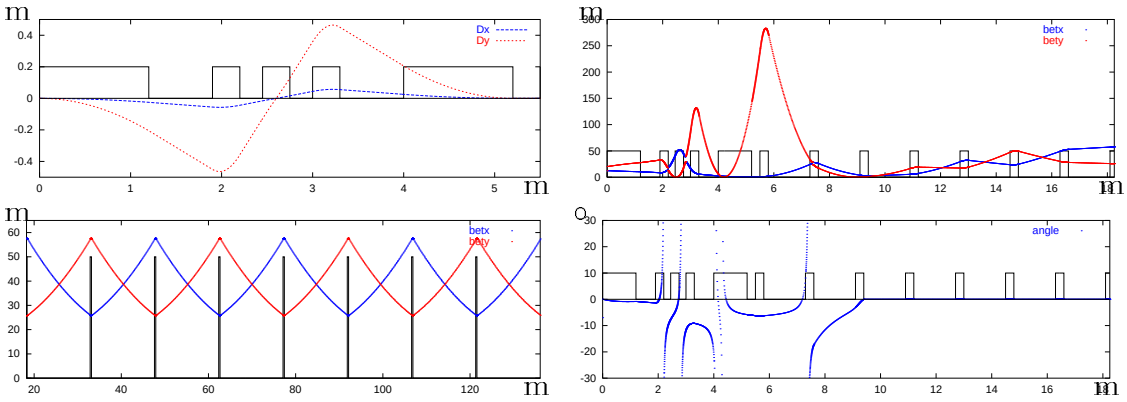

Figure 4.6: Pseudo beta functions of the coupling introduced by a tilted bend section with $\underline{M}_x = \underline{M}_y$. 1: Dispersion correction, 2 and 3: pseudo beta functions, 4: Angle Θ of the beam spot orientation.

ence of the optics.

Therefore sextupole windings inside the quadrupoles with dispersion were simulated. For the option with 5 quadrupoles between the two decoupled dipoles, four sextupole coils were added and due to the symmetry of the tilted bend section they were powered in pairs, the first sextupole having the negative strength of the fifth and the second sextupole having the negative strength of the second. For the option with 3 tilted quadrupoles between the two dipoles, the first and the last quadrupole were equipped with sextupoles which were excited asymmetrically.

5.1 Energy Dependent Emittance Increase

In figure 5.7 (top) is can be seen that transport of the phase space ellipse is strongly energy dependent whereas the origin of the ellipse does not vary much with energy. Therefore the emittance increase for the bypass with 5 horizontal quadrupoles between the decoupled bends is not strongly influenced by the higher order dispersion but it is dominated by the energy dependent Twiss parameters. The sextupoles were therefore used to minimize this effect.

When the $n \cdot \sigma$ initial phase space ellipse is described by

$$\vec{x}_i = \begin{pmatrix} x_i \\ x_i' \end{pmatrix} \ , \ \underline{\beta}_{x0} = \begin{pmatrix} \gamma_{x0} & \alpha_{x0} \\ \alpha_{x0} & \beta_{x0} \end{pmatrix} \ , \ \vec{x}_i^T \underline{\beta}_{x0} \vec{x}_i = n^2 \epsilon_x \ , \tag{5.15}$$

then after an energy dependent particle transport $\vec{x} = (\underline{M}_x + \delta \underline{M}_x^{\delta}) \vec{x}_i$ the phase space ellipse is to first order in δ described by the matrix

$$\underline{\beta}_x + \delta \underline{\beta}_x^{\delta} =_1 (\underline{M}_x + \delta \underline{M}_{x\delta})^{-T} \underline{\beta}_{x0} (\underline{M}_x + \delta \underline{M}_{x\delta})^{-1} \ . \tag{5.16}$$

Transforming the phase space ellipse for $\delta = 0$ to a circle in the normalized coordinates $\vec{x}_n$,

$$\vec{x} = \begin{pmatrix} \sqrt{\beta_x} & 0 \\ -\frac{\alpha_x}{\sqrt{\beta_x}} & \frac{1}{\sqrt{\beta_x}} \end{pmatrix} \vec{x}_n \tag{5.17}$$

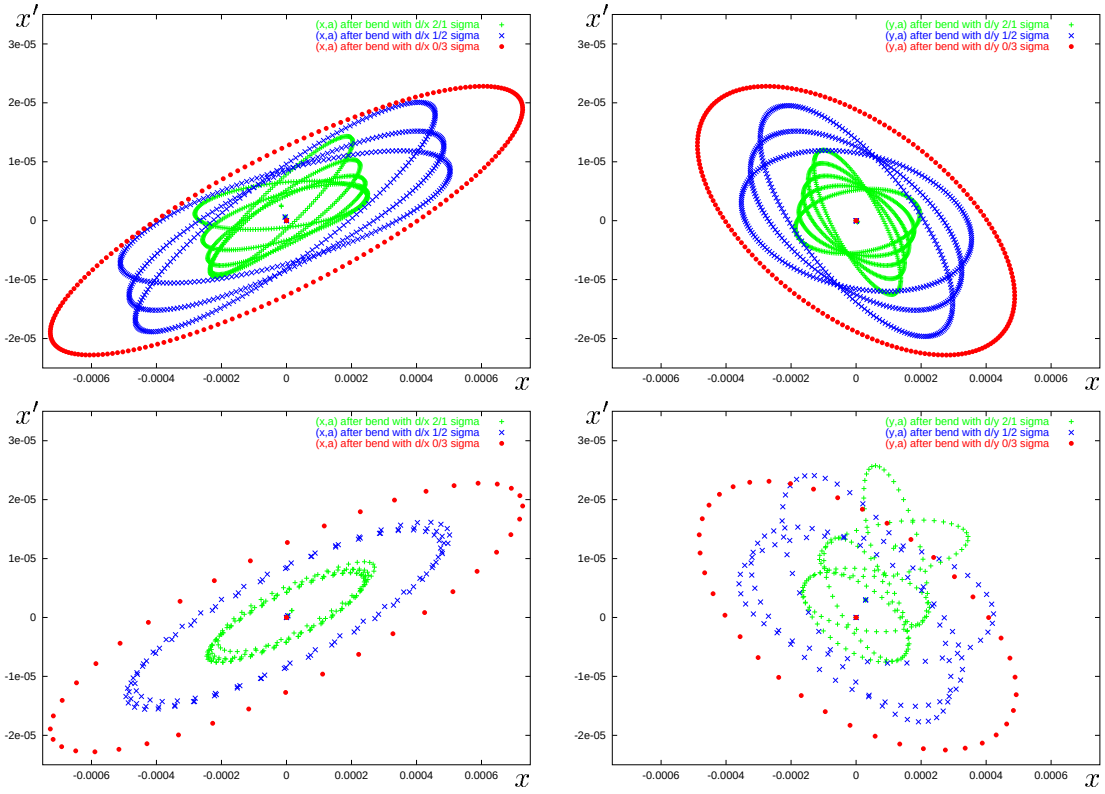

Figure 5.7: Tracking results for the tilted bend section without sextupoles for the option with 5 nearly horizontal quadrupoles between the two decoupled dipoles (top) and for the option with 3 tilted quadrupoles between the dipoles (bottom). Left: for a 1σ horizontal ellipse with ± 2, ± 1, and $0^0/_{00}$ energy deviation, a 2σ horizontal ellipse with ± 1, and $0^0/_{00}$ energy deviation, and a 3σ horizontal ellipse. Left: for a 1σ vertical ellipse with ± 2, ± 1, and $0^0/_{00}$ energy deviation, a 2σ vertical ellipse with ± 1, and $0^0/_{00}$ energy deviation, and a 3σ vertical ellipse.

leads to the ellipse

$$\vec{x}_n^T \left\{ \underline{1} + \delta \frac{1}{\beta_x} \begin{pmatrix} -\beta_x^\delta & \alpha_x^\delta \beta_x - \beta_x^\delta \alpha_x \\ \alpha_x^\delta \beta_x - \beta_x^\delta \alpha_x & \beta_x^\delta \end{pmatrix} \right\} \vec{x}_n = n^2 \epsilon_x \ , \tag{5.18}$$

where it has been used that the determinant of $\underline{\beta}_x + \delta \underline{\beta}_x^\delta =_1 1$ and therefore $\gamma_x^\delta \beta_x + \beta_x^\delta \gamma_x - 2\alpha_x \alpha_x^\delta = 0$.

Transforming to a coordinate system which is rotated by θ to lead to an upright ellipse leads to

$$\vec{x}_n = \begin{pmatrix} \cos\theta & \sin\theta \\ -\sin\theta & \cos\theta \end{pmatrix} \vec{x}_r \ , \quad \vec{x}_r^T \left\{ \underline{1} + \delta \frac{1}{\beta_x \cos(2\theta)} \begin{pmatrix} -\beta_x^\delta & 0 \\ 0 & \beta_x^\delta \end{pmatrix} \right\} \vec{x}_r = n^2 \epsilon_x \ , \tag{5.19}$$

if θ is chosen to satisfy $\beta_x^\delta \sin(2\theta) = (\alpha_x^\delta \beta_x - \beta_x^\delta \alpha_x) \cos(2\theta)$.

The area of the circle circumscribing this ellipse is therefore

$$\epsilon_{x>} = \epsilon \frac{1}{1-\delta\frac{\beta_x^\delta}{\beta_x\cos(2\theta)}} =_1 \epsilon_x + \delta\frac{\beta_x^\delta}{\beta_x\cos(2\theta)} , \tag{5.20}$$

$$\frac{d}{d\delta}\epsilon_{x>} = \frac{1}{\beta_x}\sqrt{{\beta_x^\delta}^2 + (\alpha_x^\delta\beta_x - \beta_x^\delta\alpha_x)^2} . \tag{5.21}$$

The vertical dispersion is largest in the first quadrupole as shown in figure 3.3 (a) and therefore this sextupole mostly influences the vertical emittance. After choosing this sextupole to minimize $d\epsilon_y/d\delta$, the vertical phase space ellipses change very little with energy in figure 5.8 (top right). The higher order aberrations do not distort the ellipse. This is due to the fact that the vertical beta functions are very small at the position of the sextupoles, as shown in figure 3.3 (b).

After using the sextupoles to minimize $d\epsilon_x/d\delta$, the phase space curves in figure 5.8 (top left) still change much with energy and they are shifted due to a second order dispersion. It was not possible to compensate both effects simultaneously. Additionally the ellipses are strongly distorted due to nonlinear geometric aberrations. This is due to the fact that the horizontal beta functions are large at the position of the sextupoles. In order to compensate these geometrical aberration, additional sextupoles would have to be added after a minus identity image of the linear optics. Due to these complications the tilted bend section with decoupled dipoles does not seem to be favorable.

In the emittance blowup can be computed as

$$f_{\epsilon_x} = \int_\infty \rho_0(\vec{z}_0)\vec{M}_x(\vec{z}_0)^T\underline{\beta}_x\vec{M}_x(\vec{z}_0)d\vec{z}_0 , \quad f_{\epsilon_y} = \int_\infty \rho_0(\vec{z}_0)\vec{M}_y(\vec{z}_0)^T\underline{\beta}_y\vec{M}_y(\vec{z}_0)d\vec{z}_0 . \tag{5.22}$$

Here the transport map $\vec{M}$ has been computed in different orders of expansion in $\vec{z}$ by Differential Algebra (DA) [2, 3]. During the computation advantage has been taken of the fact that for Gaussians, $\int_\infty x^{2n}\rho_0(x)dx = \sigma_x^{2n}\frac{(2n)!}{2^n n!}$, and equation (5.22) was evaluated with Differential Algebra. The following normalized emittances ϵ_x and ϵ_y are given in units of mm mrad and the energy spread σ_δ is to be given in $^0/_{00}$. The resulting averaged normalized emittances $<\epsilon_x>$ and $<\epsilon_y>$ are then given in units of mm mrad.

For the tilted bypass 5 quadrupoles between decoupled dipoles and no sextupoles,

$$\begin{aligned} <\epsilon_x> &= \epsilon_x \\ &+ 0.206\epsilon_x\sigma_\delta^2 + 0.0909\sigma_\delta^4 \end{aligned} \tag{5.23}$$

$$\begin{aligned} <\epsilon_y> &= \epsilon_y \\ &+ 0.136\epsilon_y\sigma_\delta^2 + 0.0002104\sigma_\delta^4 \end{aligned} \tag{5.24}$$

all coefficients up to order 7 are displayed which are larger than 10^{-5}. The second order dispersion influences the blowup of the horizontal emittance and the energy dependent optics blows up the emittance in both planes.

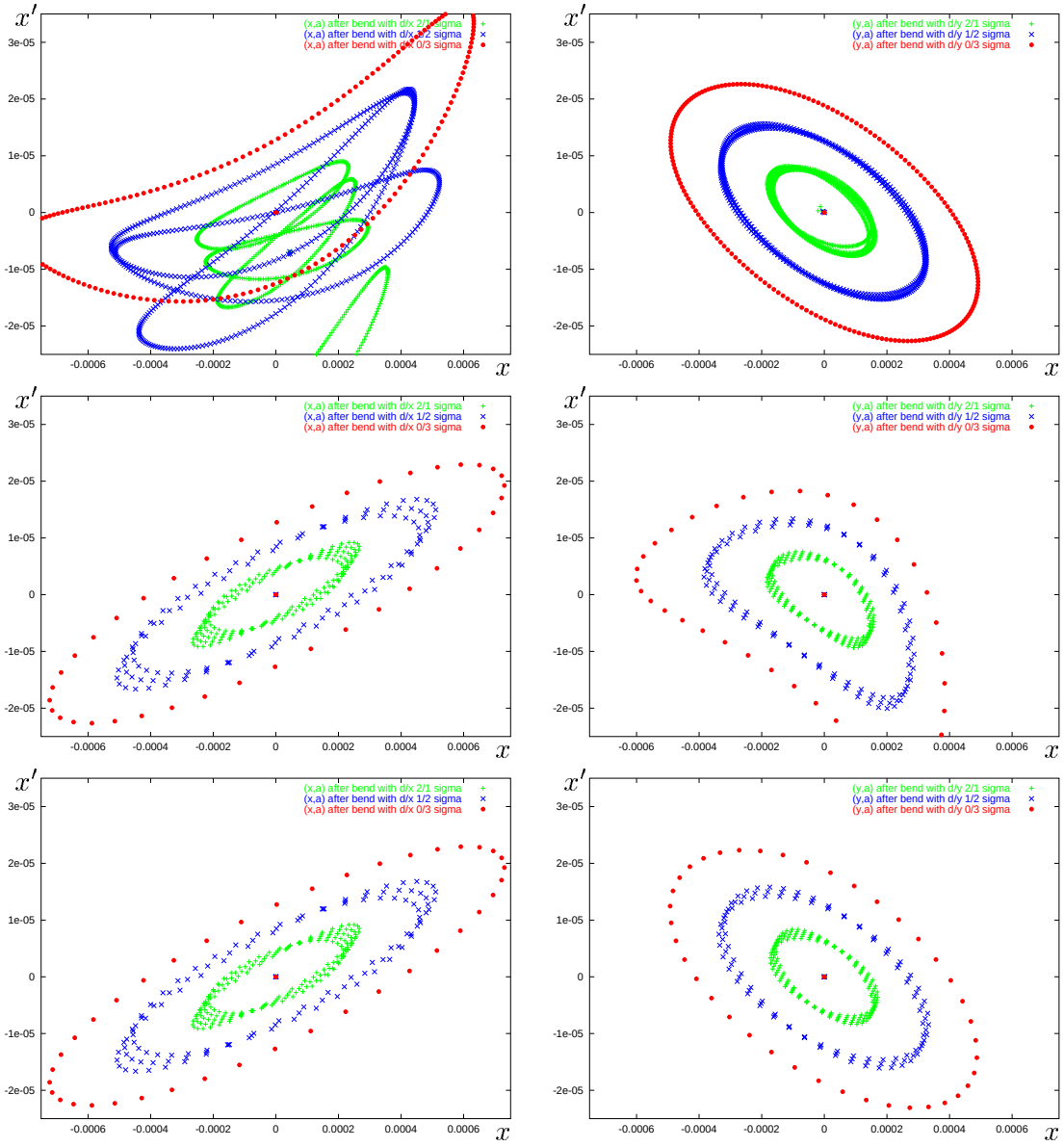

Figure 5.8: Tracking results for the tilted bend section. Top: with 5 quadrupoles between decoupled dipoles and with 4 antisymmetric sextupoles. Middle: with 3 tilted quadrupoles and an antisymmetric pair of sextupoles. Bottom: With one additional sextupole after the bend section. Left: for a 1σ horizontal ellipse with ± 2, ± 1, and $0^0/_{00}$ energy deviation, a 2σ horizontal ellipse with ± 1, and $0^0/_{00}$ energy deviation, and a 3σ horizontal ellipse. Right: for a 1σ vertical ellipse with ± 2, ± 1, and $0^0/_{00}$ energy deviation, a 2σ vertical ellipse with ± 1, and $0^0/_{00}$ energy deviation, and a 3σ vertical ellipse.

A simultaneous correction of the second order dispersion in x direction and the energy dependent phase space ellipse in x and y is not possible. The emittance

blowup corresponding to figure 5.8 (top) is

$$\begin{aligned}
<\epsilon_x> \;&= \epsilon_x \\
&+0.161\epsilon_x^2 \quad -0.143\epsilon_x\epsilon_y \quad +0.286\epsilon_y^2 \\
&-0.423\epsilon_x\sigma_\delta^2 \quad +1.23\epsilon_y\sigma_\delta^2 \quad +11.6\sigma_\delta^4 \\
&+0.00000696\epsilon_x^3 \quad -0.000185\epsilon_x^2\epsilon_y \quad +0.000626\epsilon_x\epsilon_y^2 \quad -0.0000756\epsilon_y^3 \\
&-0.0000986\epsilon_y^2\sigma_\delta^2
\end{aligned} \tag{5.25}$$

$$\begin{aligned}
<\epsilon_y> \;&= \epsilon_y \\
&+0.381\epsilon_x\epsilon_y \quad +0.000137\epsilon_y^2 \\
&+0.0149\epsilon_x\sigma_\delta^2 \quad +0.000534\epsilon_y\sigma_\delta^2 \quad +0.00209\sigma_\delta^4 \\
&+0.000268\epsilon_x^2\epsilon_y \quad -0.000308\epsilon_x\epsilon_y^2 \quad +0.0000226\epsilon_y^3 \\
&+0.0000644\epsilon_y^2\sigma_\delta^2
\end{aligned} \tag{5.26}$$

Since this emittance blowup is not tolerable, bypass with tilted quadrupoles was analyzed. Without sextupoles, corresponding to figure 5.7 (top), the emittance blowup is

$$\begin{aligned}
<\epsilon_x> \;&= \epsilon_x \\
&+0.00413\epsilon_x\sigma_\delta^2 \quad +0.000853\epsilon_y\sigma_\delta^2 \quad +0.00690\sigma_\delta^4
\end{aligned} \tag{5.27}$$

$$\begin{aligned}
<\epsilon_y> \;&= \epsilon_y \\
&+0.00000173\epsilon_x\epsilon_y \quad +0.000108\epsilon_y^2 \\
&+0.000884\epsilon_x\sigma_\delta^2 \quad +0.262\epsilon_y\sigma_\delta^2 \quad +1.176\sigma_\delta^4
\end{aligned} \tag{5.28}$$

The second order dispersion and the energy dependent optics are important in the vertical plane.

With two symmetrically arranged sextupoles for the correction of the second order dispersion one obtains

$$\begin{aligned}
<\epsilon_x> \;&= \epsilon_x \\
&+0.0000342\epsilon_x^2 \quad +0.000620\epsilon_x\epsilon_y \quad +0.000968\epsilon_y^2 \\
&+0.0186\epsilon_x\sigma_\delta^2 \quad +0.00120\epsilon_y\sigma_\delta^2
\end{aligned} \tag{5.29}$$

$$\begin{aligned}
<\epsilon_y> \;&= \epsilon_y \\
&+0.00556\epsilon_x^2 \quad -0.00251\epsilon_x\epsilon_y \quad +0.0584\epsilon_y^2 \\
&+0.00120\epsilon_x\sigma_\delta^2 \quad +0.00549\epsilon_y\sigma_\delta^2
\end{aligned} \tag{5.30}$$

The corresponding tracking result is shown in figure 5.8 (middle).

The nonlinear geometric aberrations in the vertical plane lead to a emittance blowup of about 12% which is illustrated by the strong deformation of the vertical phase space ellipse in figure 5.8 (middle right). The vertical motion is not disturbed much by the chromatic sextupoles since the horizontal pseudo beta function in figure 4.6 (b) is much smaller than the vertical at the position of these sextupoles. In order to compensate the relevant geometric aberrations, a sextupole was inserted in the dispersion free section after the second dipole. The resulting emittance blowup is

given by

$$\begin{aligned} <\epsilon_x> &= \epsilon_x \\ &+0.0000356\epsilon_x^2 \quad +0.000827\epsilon_x\epsilon_y \quad +0.0001564\epsilon_y^2 \\ &+0.0186\epsilon_x\sigma_\delta^2 \quad +0.00120\epsilon_y\sigma_\delta^2 \end{aligned} \quad , \tag{5.31}$$

$$\begin{aligned} <\epsilon_y> &= \epsilon_y \\ &+0.000602\epsilon_x^2 \quad -0.0000137\epsilon_x\epsilon_y \quad +0.000248\epsilon_y^2 \\ &+0.00120\epsilon_x\sigma_\delta^2 \quad +0.00549\epsilon_y\sigma_\delta^2 \end{aligned} \quad . \tag{5.32}$$

Also the corresponding figure 5.8 (bottom) shows that the emittance blowup is now very well corrected. The sextupole strength were fitted to minimize the relevant components of the emittance blowup by the code COSY INFINITY.

5.2 Coherent Synchrotron Radiation (CSR)

The bends which have so far been simulated with a length of 1.2 m and with an angle of 19° would produce a large emittance blowup due to coherent synchrotron radiation, as shown in figure 5.9. The effect of coherent synchrotron radiation was computed with the code TraFiC4 [4].

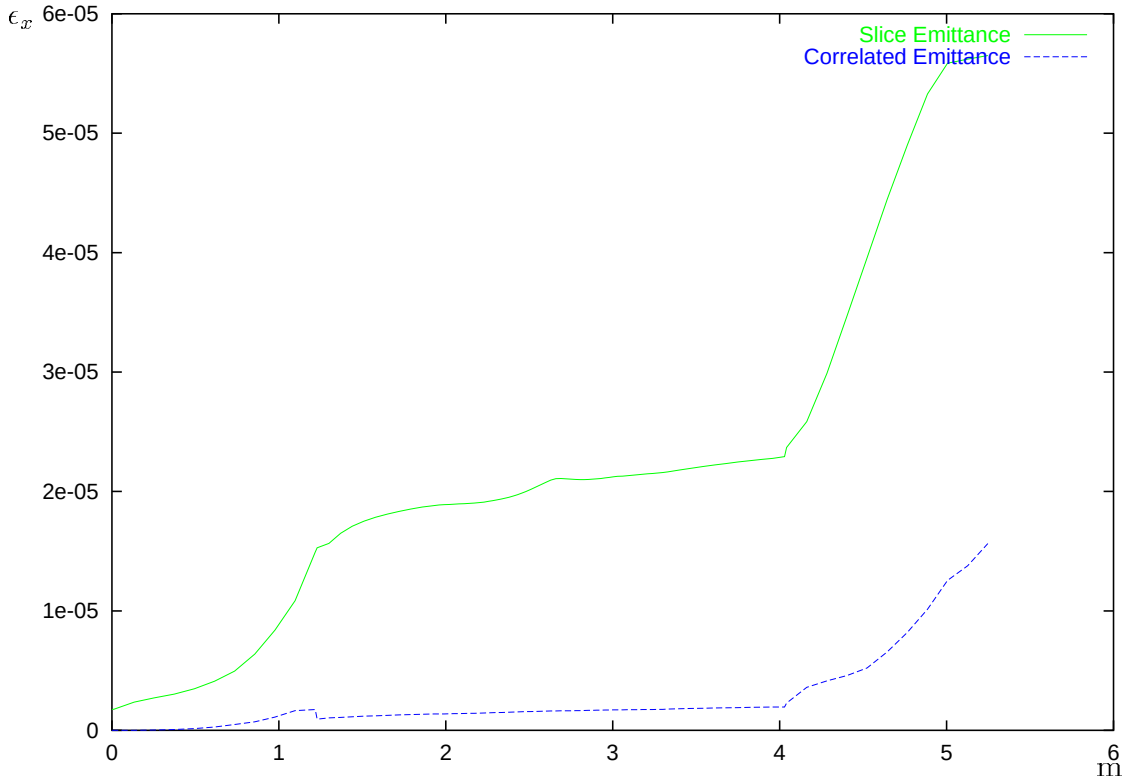

Figure 5.9: Coherent synchrotron radiation leads to an increase of the emittance by a factor about 30 when the distance between the dipole centers is 4m, the dipole length is 1.2m, and their bend angle is 19°.

Therefore the angle of the dipoles was reduced to 7° which leads to a distance of about 12 m between the dipoles. In order to lead the bypass line into the dump line after the undulators, the tilt angle between the plane of the bypass and the vertical has to be 20.445°. For these conditions the lattice was optimized and decoupled for various length of the dipoles. The increase of the projected emittance and of the emittances for beam slices with a small length is shown in figure 5.10 (left) for different dipole length. The effect of CSR has been reduced but an increase of the projected emittance by a factor of about 10 is still to large. The dependence on the dipole length is not very strong and for a dipole with 1 m length the increase of the emittance along the tilted bend section is shown in figure 5.10 (right).

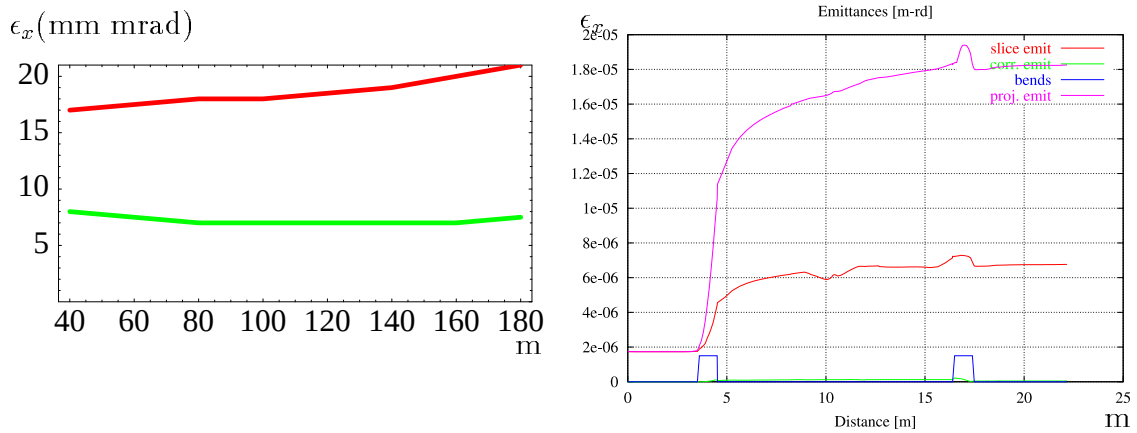

Figure 5.10: Emittance blowup after the tilted bend section due to coherent synchrotron radiation. Left: versus the length of the first two dipoles. Right: Along the bend section for 1 m long dipoles.

In order to reduce the CSR effect further, the beta functions have to be minimized in the bends. So far it had been minimized already in the second bend section and therefore the CSR effect in the second bend is much smaller than in the first. There is 89 mm of free space in the center of the 17 m module, sufficient for a quadrupole duplet. This duplet can then be used to minimize the beta functions, especially β_y, in the first bend. The design values of the Twiss parameters before this duplet are

$$\beta_{x0} = 45.63\text{m} \ , \quad \alpha_{x0} = 2.10 \ , \quad \beta_{y0} = 27.13\text{m} \ , \quad \alpha_{y0} = 0.22 \tag{5.33}$$

Figure 5.11 shows the optic of the tilted bend section after this adjustment of the beta functions.

The corresponding CSR effect is shown in figure 5.12 (left). An increase of the projected emittance by about a factor of 4.5 for a 1 GeV beam is marginally acceptable. For smaller energies the CSR increases the projected emittance by larger factors as shown in figure 5.12 (right). The beta functions of $\beta_x = 45.63$ and $\beta_y = 27.13$ at the duplet inside the 17 m module could be increased by changing the optics further upstream. Then the beta functions in the first bend could be further reduced, leading to a further reduction of the emittance blowup due to CSR.

For the optics shown in figure 5.11,the nonlinear emittance transport is quite unproblematic. As shown in equation (5.34), the emittance is very little influenced

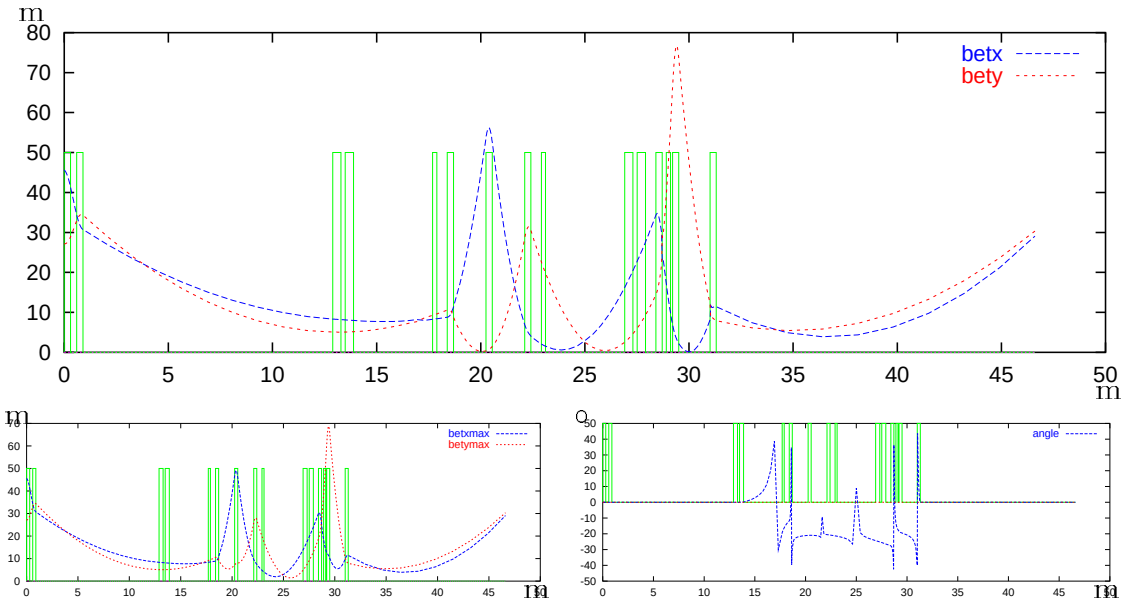

Figure 5.11: a) Pseudo beta functions, b) beta functions taken from the maximal horizontal and vertical extension of the beam spot, and c) the angle of the beam spot in the tilted section after adjustment of two quadrupoles before this section.

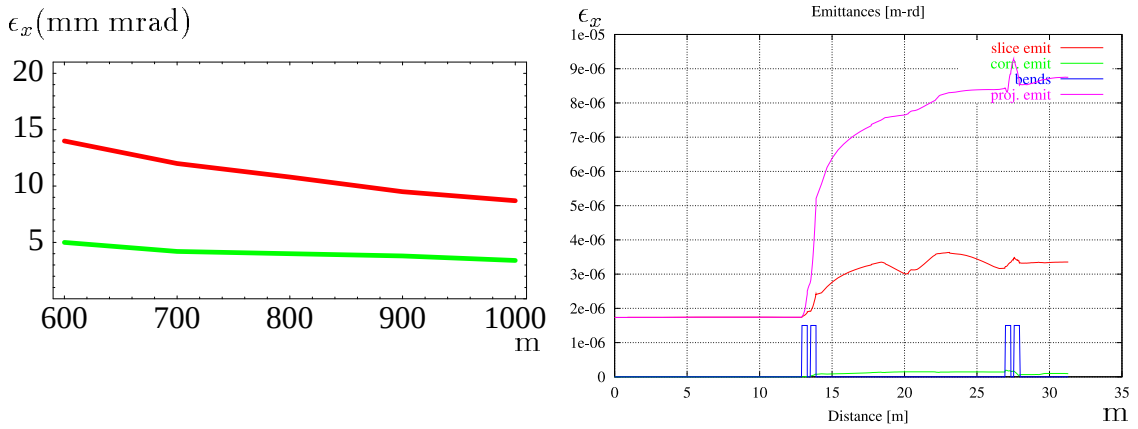

Figure 5.12: Left: CSR effect for different beam energies. Right: CSR emittance blowup along the tilted section after adjustment of two quadrupoles before this section for a 1 GeV beam.

by nonlinear motion. As in equation (5.24) the normalized emittances are to be taken in units of mm mrad and the energy spread in units of $^0/_{00}$. For the design emittance of 2 mm mrad the largest effect of 2% is due to the second order dispersion. After this dispersion is corrected by a tilted pair of antisymmetric sextupoles in the tilted bend section, the blowup is given by equation (5.35). These sextupoles were taken to be 0.2 m long with a strength of $\mp 8.94/\mathrm{m}^2$. The small nonlinear effect proportional to $\epsilon_x\epsilon_y$ amounts only to 0.02% and does not need to be corrected. It

could be corrected by an additional tilted sextupole 1 m after the tilted bend section with $2.27/\mathrm{m}^2$, as shown in equation (5.36).

$$\begin{aligned} <\epsilon_x> &= \epsilon_x + 0.0021\epsilon_x\sigma_\delta^2 + 0.0001\epsilon_y\sigma_\delta^2 + 0.0063\sigma_\delta^4 \qquad (5.34)\\ <\epsilon_y> &= \epsilon_y + 0.0001\epsilon_x\sigma_\delta^2 + 0.0023\epsilon_y\sigma_\delta^2 + 0.0395\sigma_\delta^4 \\ <\epsilon_x> &= \epsilon_x + 0.0026\epsilon_x\sigma_\delta^2 + 0.0003\epsilon_y\sigma_\delta^2 \qquad (5.35)\\ <\epsilon_y> &= \epsilon_y + 0.0003\epsilon_x\sigma_\delta^2 + 0.0005\epsilon_y\sigma_\delta^2 + 0.0001\epsilon_x\epsilon_y \\ <\epsilon_x> &= \epsilon_x + 0.0026\epsilon_x\sigma_\delta^2 + 0.0003\epsilon_y\sigma_\delta^2 \qquad (5.36)\\ <\epsilon_y> &= \epsilon_y + 0.0003\epsilon_x\sigma_\delta^2 + 0.0005\epsilon_y\sigma_\delta^2 \end{aligned}$$

For the proposed optics the sextupoles are not needed to transport a beam with design energy spread and design emittance. If one wants to be flexible to handle larger beta functions in the dispersive region and larger energy spreads, then the three sextupoles could be installed. The small emittance blowup due to nonlinear motion is illustrated by the tracking pictures of figure 5.13.

5.3 Further Requirements

Inside the bypass line there should be a beam spot which is smaller than 150 μm$\times$150 μm to test materials under electron bombardment. The optics starting after the second bend is shown in figure 5.14 (top) for a spot with beta functions of 1 m and in 5.14 (bottom) for a spot with beta functions of 4 m. For a 1 GeV beam this corresponds to a tunable spot size of 71 μm to 143 μm assuming an emittance which has blown up to 10 mm mrad.

It is planed to use the last tilted dipole in the bypass line, which bends the beam down into the dump, as a spectrometer magnet. Therefore there should be a small beam diameter in the dispersive plane in order to optimize the energy resolution. For this reason, the quadrupole just in front of this dipole also has to be tilted. Figure 5.15 shows the beta functions of equation (3.14) corresponding to the maximal extension of the beam spot of the coupled motion where x refers to the dispersive plane. The last two quadrupoles are also tilted and can be used for the beam coming form the bypass beam line as well as for the beam from the main beam line which is also directed into the dump by a tilted dipole magnet.

The magnets of the complete beam line are specified in table 5.1.

References

[1] M. Berz, K. Makino, K. Shamseddine, G. H. Hoffstaetter, and W. Wan, COSY INFINITY and its applications in nonlinear dynamics, in *Computational Differentiation, Techniques, Applications, and Tools*, pp. 363–367, SIAM (1996)

[2] M. Berz, Differential Algebra–a new tool, *Report***LBL-27033**, Lawrence Berkeley Laboratory (1989)

Element	Length	Strength	Tilt	Adjacent Drift
Quad	0.3 m	0.7834179/m	0°	0.3 m
Quad	0.3 m	-0.9187773/m	0°	11.662 m
Dipole	0.4 m	3.5°	69.555°	0.2 m
Dipole	0.4 m	3.5°	69.555°	4.5 m
Quad	0.3 m	2.5316110/m	69.555°	1.5625 m
Quad	0.3 m	-2.4706471/m	69.555°	1.5625 m
Quad	0.3 m	2.5316110/m	69.555°	4.5 m
Dipole	0.4 m	−3.5°	69.555°	0.2 m
Dipole	0.4 m	−3.5°	69.555°	0.5 m
Quad	0.3 m	-3.7223654/m	69.555°	0.5 m
Quad	0.3 m	3.7781409/m	69.555°	1.5 m
Quad	0.3 m	-3.4149135/m	69.555°	17.0 m
Quad	0.3 m	2.1940838/m	0°	1.0 m
Quad	0.3 m	-4.7027817/m	0°	2.0 m
Quad	0.3 m	-4.0713551/m	0°	1.0 m
Quad	0.3 m	2.0081454/m	0°	17.0 m
Quad	0.3 m	-0.109159/m	0°	17.0 m
Quad	0.3 m	0.2047387/m	0°	17.0 m
Quad	0.3 m	0.3875800/m	83°	3.482 m
Dipole	1.2 m	−19°	83°	7.137 m
Quad	0.3 m	-2.0000000/m	83°	2.873 m
Quad	0.3 m	-0.7000000/m	83°	3.7 m

Table 5.1: Magnets in the TTF2 bypass line.

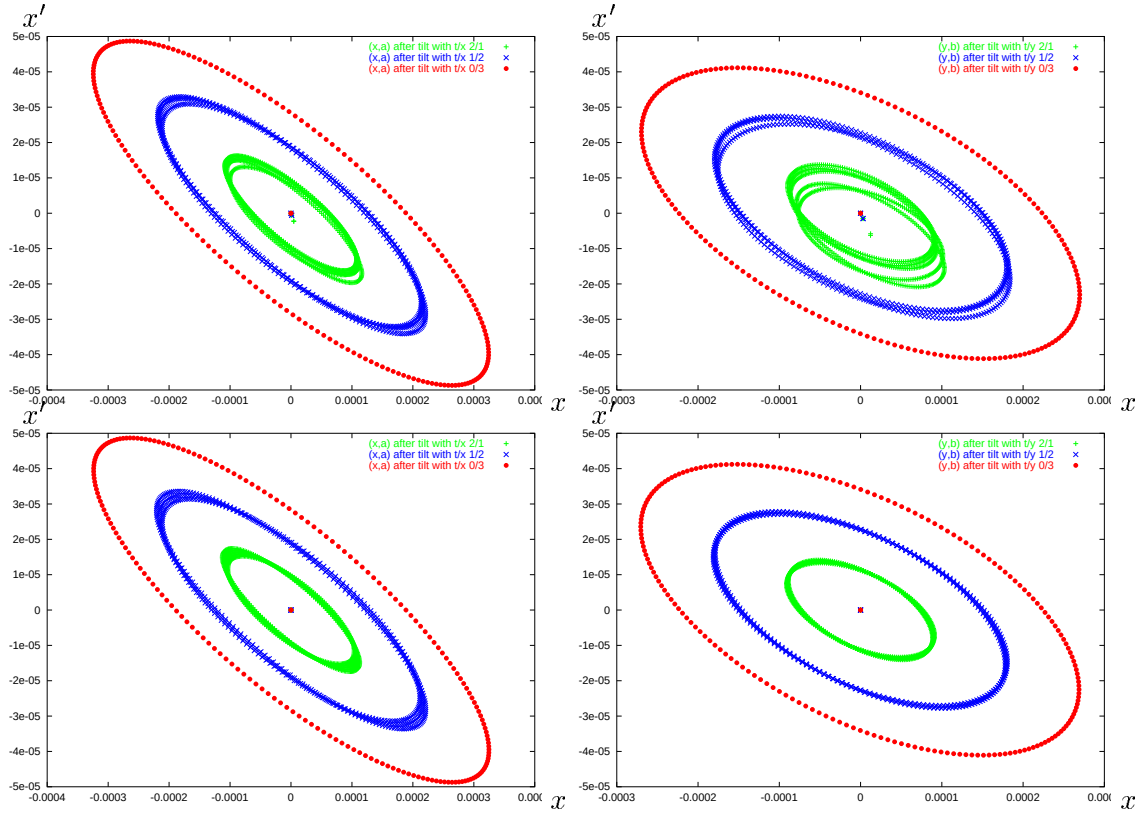

Figure 5.13: Tracking results for the tilted bend section of the TTF2 bypass as specified in table 5.1. Top: without sextupoles. Bottom: with two asymmetric sextupoles in between the bends the second order dispersion. Left: for a 1σ horizontal ellipse with ± 2, ± 1, and $0^0/_{00}$ energy deviation, a 2σ horizontal ellipse with ± 1, and $0^0/_{00}$ energy deviation, and a 3σ horizontal ellipse. Right: for a 1σ vertical ellipse with ± 2, ± 1, and $0^0/_{00}$ energy deviation, a 2σ vertical ellipse with ± 1, and $0^0/_{00}$ energy deviation, and a 3σ vertical ellipse.

[3] M. Berz, Arbitrary Order Description of Arbitrary Particle Optical Systems, *NIM***A298**, pp. 426–440 (1990)

[4] M. Dohlus, A. Kabel, T. Limberg *NIM***A445**, pp. 338-342 (2000)

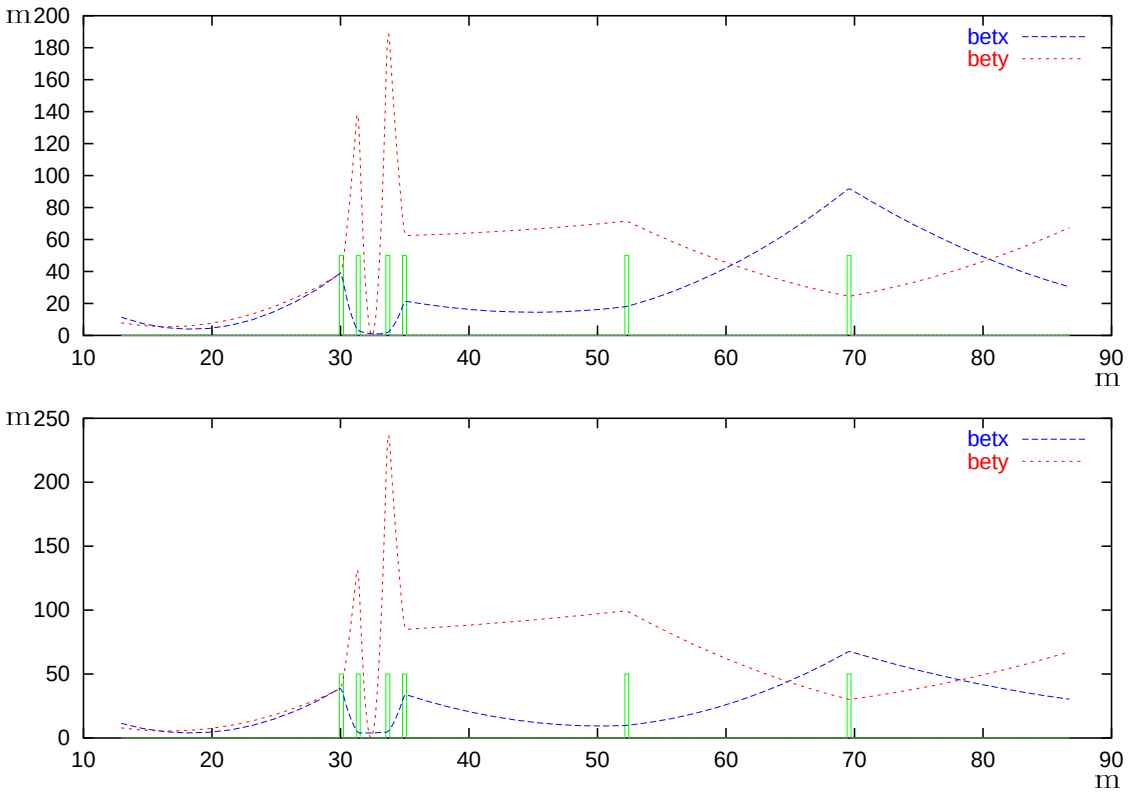

Figure 5.14: Beta functions for the bypass after the tilted magnets. The focus is in the center between the two duplets which are separated by 2 m. Top: for a section with $\beta_x = 1$ m and $\beta_y = 1$ m. Bottom: for a section with $\beta_x = 4$ m and $\beta_y = 4$ m.

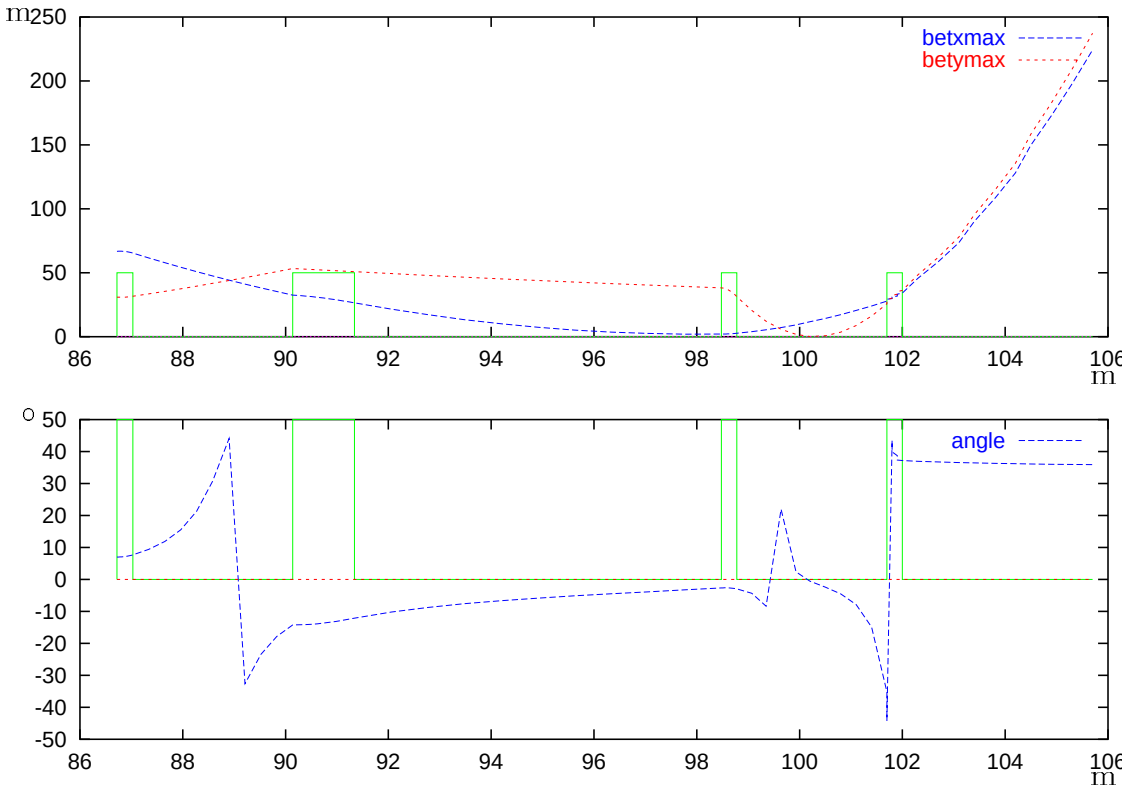

Figure 5.15: Top: The beta functions corresponding to the maximal extension of the beam spot for the dispersive plane (x)and for a plane transverse to it (y). Bottom: The tilt angle of the beam ellipse.